moni, L. Sabbatini, P. G. Zambonin, and G. Caporiccio, *Thin Solid Films*, **143,** 163 (1986).
9. X. C. Mu, S. J. Fonash, G. S. Oehrlein, S. N. Chakravarti, C. Parks, and J. Keller, *J. Appl. Phys.*, **59,** 2958 (1986).
10. P. Launay, G. Turban, B. Grolleau, and C. de Prost, *Le Vide—Les couches minces,* 218 suppl., 107 (1983).
11. G. Turban, B. Grolleau, P. Launay, and P. Briaud, *Rev. Phys. Appl.*, **20,** 609 (1985).
12. G. Turban and M. Rapeaux, *This Journal,* **130,** 2231 (1983).
13. S. I. Raider and R. Flitsch, *ibid.*, **123,** 1754 (1976).
14. S. I. Raider and R. Flitsch, *IBM J. Res. Dev.*, **22,** 294 (1978).
15. D. T. Clark, W. J. Feast, D. Kilcast, and W. K. R. Musgrave, *J. Polym. Sci.*, **11,** 389 (1973).
16. D. T. Clark, W. J. Feast, I. Ritchie, and W. K. R. Musgrave, *J. Polym. Sci. Polym. Chem. Ed.*, **12,** 1049 (1974); D. T. Clark, "Structure, Bonding and Reactivity of Polymer Surfaces Studied by Means of ESCA," C.R.C. Critical Reviews in Solid State and Material Science, p. 1 (1978).
17. D. T. Clark, *Phys. Scr.*, **16,** 307 (1977).
18. C. R. Ginnard and W. M. Riggs, *Anal. Chem.*, **44,** 1310 (1972).
19. G. S. Oehrlein, J. G. Clabes, and P. Spirito, *This Journal,* **133,** 1002 (1986).
20. C. D. Wagner, W. M. Riggs, L. E. Davis, J. F. Moulder, and G. E. Muilenberg, "Handbook of X-Ray Photoelectron Spectroscopy," Perkin Elmer Corp. (1979).
21. D. W. Rice and D. F. O'Kane, *This Journal,* **123,** 1308 (1976).
22. D. T. Clark, W. J. Feast, W. K. R. Musgrave, and I. Ritchie, *J. Polym. Sci. Polym. Chem. Ed.*, **13,** 857 (1975).
23. A. Dilks and E. Kay, *Macromolecules,* **14,** 855 (1981).
24. D. T. Clark and D. Shuttleworth, *J. Polym. Sci. Polym. Chem. Ed.*, **17,** 1317 (1979).
25. D. A. Shirley, *Phys. Rev.*, **B5,** 4709 (1972).
26. D. W. Marquardt, *J. Soc. Ind. Appl. Math.*, **11,** 431 (1963).
27. J. H. Thomas III and G. Kaganowicz, *Mat. Res. Soc. Symp.*, Proc. Vol. **38,** 293 (1985).
28. F. J. Grunthaner, P. J. Grunthaner, R. P. Basquez, B. F. Lewis, and J. Maserjian, *J. Vac. Sci. Technol.*, **16,** 1443 (1979).
29. G. Hollinger and F. J. Himpsel, *Appl. Phys. Lett.*, **44,** 93 (1984).
30. M. P. Seah, "Practical Surface Analysis by Auger and XPS," E. Briggs and M. P. Seah, Editors, p. 181, Wiley (1983).
31. M. P. Seah and W. A. Dench, *Surf. Interface Anal.*, **1,** 2 (1979).
32. D. R. Penn, *J. Electron. Spectrosc. Relat. Phenom.*, **9,** 29 (1976).
33. J. Szajman and R. C. G. Leckey, *J. Electron. Spectrosc. Relat. Phenom.*, **23,** 80 (1981).
34. G. J. Coyle and G. S. Oehrlein, *Appl. Surf. Sci.*, **25,** 423 (1986).
35. I. Solomon, M. P. Schmidt, M. Driss Khodja, and C. Sénémaud, To be published.
36. C. Cardinaud, A. Rhounna, G. Turban, and B. Grolleau, "Le Vide—Les Couches minces," 237 suppl, 133 (1987).
37. G. S. Oehrlein, R. M. Tromp, J. C. Tsang, Y. H. Lee, and E. J. Petrillo, *This Journal*, **132,** 1441 (1985).

Polyimide Film Properties and Selective LPCVD of Tungsten on Polyimide

R. W. Pattee, C. M. McConica, and K. Baughman

Colorado State University, Fort Collins, Colorado 80523

ABSTRACT

du Pont PI-2575-D polyimide films were characterized to determine their suitability for use as an interlevel dielectric with a selective tungsten via fill process. Polyimide films cured at 400° and 440°C were found to breakdown at voltages greater than 1×10^6 V/cm. The pinhole density, when processed in a non-cleanroom environment, is below 1 per cm^2. The dielectric constant for 1.6 μm films is 3.9. Adhesion to thermal oxide is 100% for films in boiling water up to 1h. The maximum moisture absorption is 1.7 w/o at 90% relative humidity. Perfect tungsten selectivity was achieved in the absence of nearby tungsten surfaces at 216°C, 0.75-7.5 torr total pressure, 15:1 H_2:WF_6 and times to 210 min. When the polyimide was exposed to adjacent tungsten surfaces, tungsten did deposit on the polyimide, resulting in a moving metal front. The activation energy for the rate of progress of the tungsten film front is 16 kcal/mol.

The microelectronics industry has demonstrated several applications for polyimides in recent years, including alpha-particle barriers in high density memory devices, passivation and protection layers, interlevel dielectrics, and ion implantation masks (1). As the size of integrated circuit elements has decreased, the fraction of chip area taken up by interconnect has increased. To reduce chip size and improve performance, IC researchers have moved toward multilevel metal interconnects. MIT's Lincoln Laboratory (2), Texas Instruments (3), TRW Inc. (4), Honeywell (5), and Nippon Telephone and Telegraph (6) have all reported multilevel metal processes that use polyimides, rather than inorganic materials, as the interlevel dielectric.

Additionally, CVD tungsten has recently proven useful in microelectronics; applications include contact barriers (7), selective via fill (8), and low resistance shunts on MOS gate and source/drain areas (9). In the case of selective deposition, tungsten will deposit preferentially on silicon, metals, and metal silicides, with no deposition on silicon dioxide and other insulators. A selective tungsten deposition process is desirable in the case of contact barriers, via fill, and MOS shunts because the process is self-patterning (*i.e.*, no lithography and etching steps are needed).

A number of studies have been carried out to examine the selective deposition of tungsten on inorganic dielectrics such as silicon dioxide and silicon nitride (7-11). Since polyimides are being introduced as a replacement for inorganic dielectrics in multilevel IC applications, it follows that a selective tungsten process, such as selective fill of polyimide vias between metal levels, would be very desirable.

The first goal of this research was to characterize a commercially available polyimide, to assess its suitability for use as an interlevel dielectric. The characterization tests included film thickness parameters, film adhesion, pinhole density, moisture absorption, dielectric constant, and dielectric breakdown strength. The second goal was to carry out an initial study of LPCVD of tungsten on polyimide, to determine whether polyimide can act as a selective surface (free of tungsten deposition). Once it was determined that the polyimide is selective under certain conditions, factors that caused the loss of selectivity were examined. Finally, the nonselective tungsten film growth on the polyimide was characterized. du Pont's PI-2757-D, a new generation PI formulation with a built-in aminosilane adhesion promoter, was chosen for this work.

Downloaded on 2015-06-14 to IP 134.117.10.200 address. Redistribution subject to ECS terms of use (see ecsdl.org/site/terms_use) unless CC License in place (see abstract).

Equipment

For the polyimide film preparation, a Solitec 4110 wafer spinner was used. The films were not prepared in a cleanroom environment; instead a Plexiglas glove box covered the spinner to minimize the presence of particles. Desiccated air, filtered to 1 μm, was passed into the chamber to keep the humidity below 30% RH. The spinner's exhaust blower was used to vent solvent fumes and to prevent formation of an aerosol fog of polyamic acid particulates above the wafer's surface.

A hot plate was used in conjunction with a Blue M convection oven to soft bake the polyimide films. For the imidization (curing) step a vacuum curing furnace was built which consisted of a 135 mm ID horizontal quartz tube with a 30 cm "hot zone." A Welch Duo-Seal vacuum pump was used to pull high purity nitrogen through the furnace while pressure was manually controlled with a gas rotameter at the furnace inlet. The furnace temperature was ramped from ambient to the specified temperature over a desired time using a PID temperature controller.

PI film thickness and thickness uniformity were measured with a Tencor Alpha-Step 100 profilometer. A Plexiglas constant humidity chamber, in conjunction with a sensitive Mettler balance (readable to 0.00001g) was used for moisture absorption measurements. ASTM method D-3359 (12) was used as the standard for semiquantitative tape peel adhesion tests. A mercury probe and capacitance meter were used to measure dielectric constant at a 1 MHz ac signal, and dielectric breakdown field strength was measured using an I-V curve tracer. Pinhole density was determined using a methanol bubbling apparatus and a stereomicroscope. The bubbler consisted of a 10 cm glass petri dish with a wire ring electrode suspended above an aluminum plate in methanol. The test wafer sat on top of the plate electrode and below the wire ring.

For the tungsten deposition studies, a low pressure, single wafer, cold wall CVD reactor was built; it is shown schematically in Fig. 1. It replaced the original research reactor built by Krishnamani (11) and was designed to meet the following objectives: (*i*) uniform substrate heating, (*ii*) cool reactor walls for minimal wall deposition, (*iii*) 100 mm wafer capability, (*iv*) more accurate substrate temperature measurement, (*v*) no polymer seals (for higher temperature operation), (*vi*) view port flange (for visual wafer inspection during deposition).

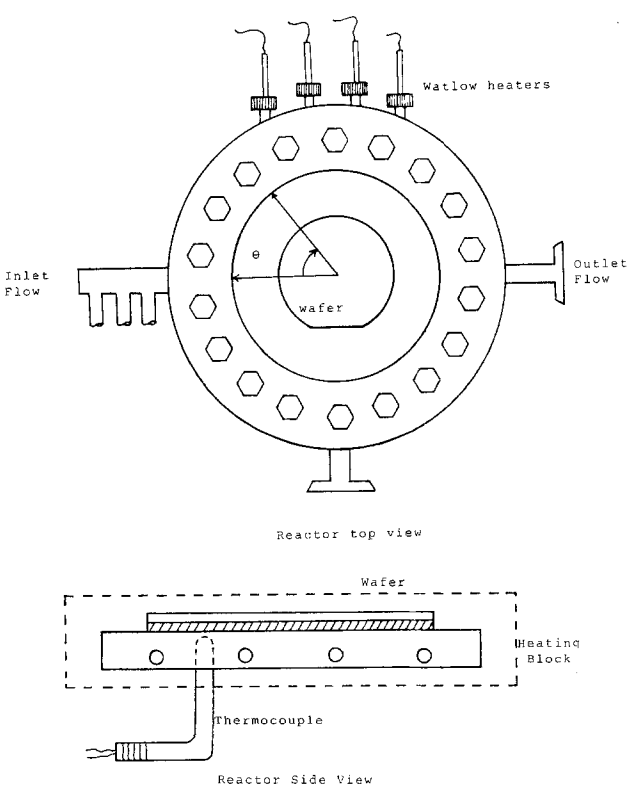

Fig. 1. Vertical and side view of flanged reactor. Angle denotes angle from inlet at 0°.

The reactor was built from three 17.1 cm 304 stainless steel flanges bolted together with OFHC copper gaskets. The top flange, fitted with a 10 cm glass view port and Kovar seal, serves as both the reactor door and viewing window. The center flange is hollow and accommodates a 1.0 cm thick, 11.4 cm diameter OFHC copper heating block for conductive substrate heating. Four Watlow Firerod resistive cartridge heaters are fitted into the block, with a uniformly distributed power output of 530W. A thermowell is machined into the bottom of the block, midway between two rods. The well comes within 0.13 cm of the top surface of the heating block, and a sheathed type K thermocouple fits snugly into this well. Since the copper block contacts the reactor walls only via the poorly conductive heating rods and thermocouple, the walls are considerably cooler than the substrate. The copper block is completely coated with tungsten from the first few deposition runs. Reactant gases flow from left to right across the reactor, parallel to the substrate. Actual wafer surface temperatures were determined by cementing an Omega thin film resistance temperature detector (no. TFD-M) to the polyimide surface on a test wafer under actual deposition conditions.

The gas handling equipment, mass flow controllers, temperature controller, and vacuum pumping station for the reactor were essentially the same as those described by McConica (13). Ultrapure tungsten hexafluoride (99.9%), donated by Genus Incorporated, was used for this study.

Experimental Procedure

P-type (100) 50 mm polished silicon wafers were used as the substrate for the polyimide film preparation and characterization. Each wafer was first put through a dehydration bake for 30 min at 180°C and then centered on the spinner chuck. PI-2575-D polyamic acid solution was poured directly from the bottle onto the wafer surface, forming a puddle that covered half the wafer area. After a brief spread cycle at 500 rpm, the spinner was programmed to ramp quickly to the desired spin speed and maintain that speed for 30s. Spin speeds ranged from 2000 to 8000 rpm.

The soft-bake procedure that yielded the best overall film appearance and uniformity was a 60s/90°C hot-plate bake followed by an 8 min/150°C convection oven bake. The back-side heating of the wafer (via hot plate) immediately following a spin appeared to provide a good degree of reflow, resulting in a more uniform film.

The films were cured by ramping them from ambient to 400°C in 2h, holding at 400°C for 20 min, then ramping back down. At temperatures above 350°C, the films were cured in a 10 torr nitrogen atmosphere. For best adhesion, the manufacturer recommends that the films be cured in air at temperatures below 350°C (14).

Cured film thicknesses were measured by making three cuts in the PI film, 2 cm long and 1.5 cm apart. An Alpha-Step thickness measurement was made near the ends of each cut. Six measurements on each of three identically prepared wafers were made to determine thickness uniformity across a given wafer and from wafer-to-wafer.

For the moisture absorption test, a thick coat (7.3 μm) of polyimide was applied to two wafers during two successive 2000 rpm spins. The two wafers were placed in the constant humidity chamber and allowed to absorb water until equilibrium at a given wet bulb temperature (*i.e.*, relative humidity) was reached. This was typically in less than 10 min. The wafers were then weighed to the nearest 0.00001g and returned to the chamber. Each wafer was weighed three times at each of the eight humidity levels between 0 and 85% RH. The average net moisture gain was reported as a percentage of polyimide film mass.

Three wafers were used for the tape peel adhesion tests. After cure, a grid of six horizontal and six vertical lines were cut into the film with a sharp blade and straight edge. The lines were about 7 mm long and 1 mm apart, making a grid of twenty-five 1 mm^2 squares. A fresh piece of Scotch brand tape no. 104 was applied over the grid, rubbed down

Downloaded on 2015-06-14 to IP 134.117.10.200 address. Redistribution subject to ECS terms of use (see ecsdl.org/site/terms_use) unless CC License in place (see abstract).

Table I. du Pont PI-2575-D test results

Film property	400°C cure Observed	400°C cure Reported	440°C cure Observed	Silicon dioxide (21)	Silicon nitride (21)
Dielectric constant	3.9	4.5	3.7	3.9	7.5
Dielectric breakdown strength, MV/cm	>1.0	2.4	>1.0	~5	~10
Cured film density g/cm^3	1.45	1.41		2.2	3.1
Thickness loss during cure, %	23	22	24		
Film thickness uniformity					
across wafer, %	1				
wafer-to-wafer, %	1				
Adhesion loss, % area nonadherant; 3 wafer samples					
Ambient cond.	0, 0, 0	0	0, 0, 0		
1h boiling H_2O	0, 2, 0	0	0, 0, 0		
2h boiling H_2O	0, 77, 0	0	4, 10, 0		
Maximum moisture uptake, w/o at 90% RH	1.7	~3			
Pinhole density, cm^{-2}	0.9		0.7		

firmly with an eraser, and then slowly peeled back. An estimate of the percentage of grid area removed by the tape was then made. The test was repeated after the wafers sat in room temperature DI water for 15 min. It was repeated again after 15 min, 1h, and 2h in boiling DI water. The tests were then repeated after the wafers were recured at 440°C.

Two wafers were used for the pinhole count. After cure, each wafer was placed in the methanol bubbler such that the wafer's back side made good electrical contact with the bottom electrode. A variable voltage was applied between the wafers and the ring electrode and was increased slowly until microscopic bubbles appeared from pinholes in the PI film surface. The pinholes were counted over three different 3.9 cm^2 areas on each of the two wafers, and the results were averaged. The test was repeated after the 440°C cure.

The procedure for the selective tungsten deposition study called for isolating the polyimide films from hot tungsten surfaces present in the reactor. In the case of silicon dioxide, it has been found that nearby hot tungsten acts as a catalyst for tungsten nucleation and eventual film growth on SiO_2 (13, 15). Teflon was chosen as the material to isolate the polyimide coated wafers from the tungsten coated heating block. Under the conditions of 0.75 torr total pressure, 216°C reactor (60°C below significant Teflon outgassing), and 15:1 H_2:WF_6 flow ratio, it has been observed that tungsten does not deposit on Teflon.

P-type (001) 75 mm polished silicon wafers were used as the substrate for the PI selectivity study. The wafers were thermally oxidized to a thickness of 154 nm so that there were no exposed silicon surfaces upon which tungsten would deposit. Thin polyimide films (1.7 μm after cure) were prepared according to the previously described procedure and then stored in a desiccator. For each deposition run, a thin sheet of Teflon (0.01 cm) was fitted snugly over the tungsten-coated reactor heating block, and the PI coated wafer was then centered on the Teflon. For the tests on Teflon, reactor temperature was maintained at 216°C, H_2:WF_6 flow ratio was 15:1, total flow was 160 sccm, and total pressure was either 0.75 or 7.5 torr. Deposition times ranged from several minutes to several hours. Each wafer was weighed to the nearest 0.00001g before and after a run to determine the extent of tungsten deposition.

For the nonselective tungsten deposition, the Teflon barrier was not used. A 75 mm oxidized wafer was centered on the tungsten-coated heating block, and the PI-coated test wafer was placed on top of the oxidized wafer. This stacking minimized the back-side tungsten deposition that occurs when an oxidized wafer is in contact with the heating block. Hydrogen was flowed through the reactor at 150 sccm and the wafer temperature (216°, 243°, 268°, 293°C) and pressure (0.75 torr) were allowed to stabilize. At time zero, WF_6 was metered into the reactor at 10 sccm. The progress of the nonselective tungsten growth sequence was photographed through the view port flange with a 35 mm camera and wide angle lens.

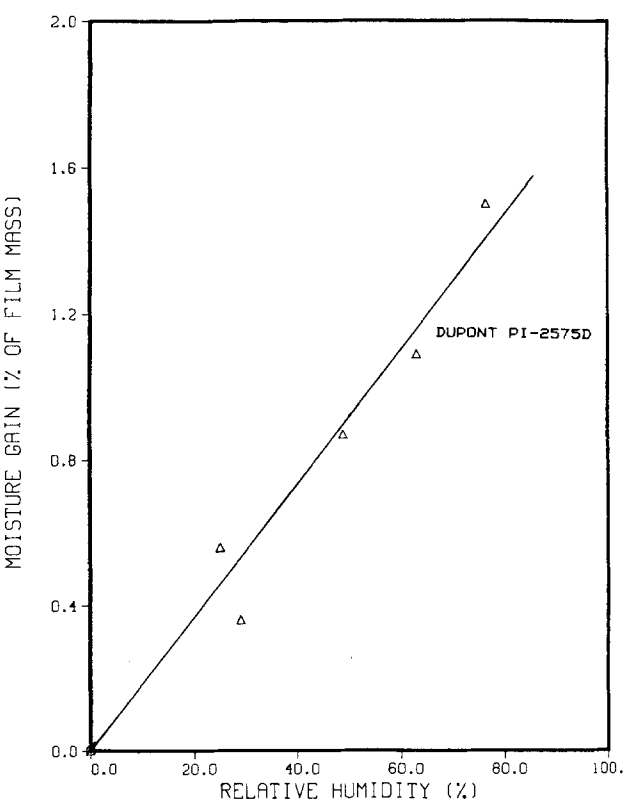

Fig. 2. Moisture gain as a function of relative humidity

Results

Table I summarizes the results for the polyimide film testing, as well as reported values from the manufacturer and equivalent properties of silicon dioxide and silicon nitride, where applicable.

A good log-log correlation between cured film thickness and spin speed was observed for this material. Polyimide moisture gain was found to be linearly dependent on relative humidity; the results are shown in Fig. 2.

From the selective deposition study, it was found that no tungsten deposited on the polyimide for deposition times of 90-210 min at 0.75 torr total pressure and 216°C. Additionally, there was no deposition after 93 min at 7.5 torr. None of the wafers exhibited any mass change. There were no changes in the dark green PI film or in the royal blue SiO_2 film on the back sides of the wafers.

Unlike the runs made with the Teflon heating block cover, tungsten readily deposited on the PI films once the Teflon was removed. During each of the four runs, no visible deposition was observed immediately after the start of the reaction. After approximately 1 (293°C)-13 min (216°C), tungsten began to appear on the PI surface at the wafer edge nearest the reactor inlet (≤0°). The tungsten film edge started moving radially inward from 0° and covered

Downloaded on 2015-06-14 to IP 134.117.10.200 address. Redistribution subject to ECS terms of use (see ecsdl.org/site/terms_use) unless CC License in place (see abstract).

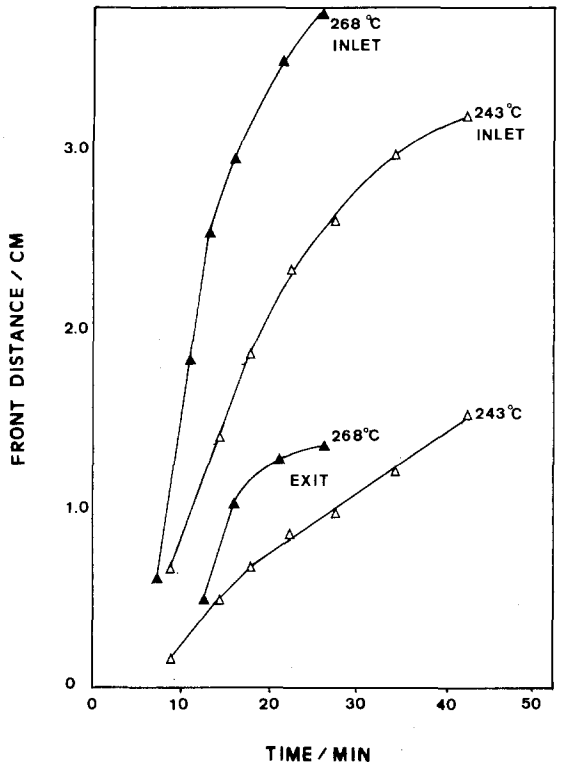

Fig. 3. Tungsten front distance from wafer edge at inlet side (0°) and exit side (180°) as a function of time and temperature.

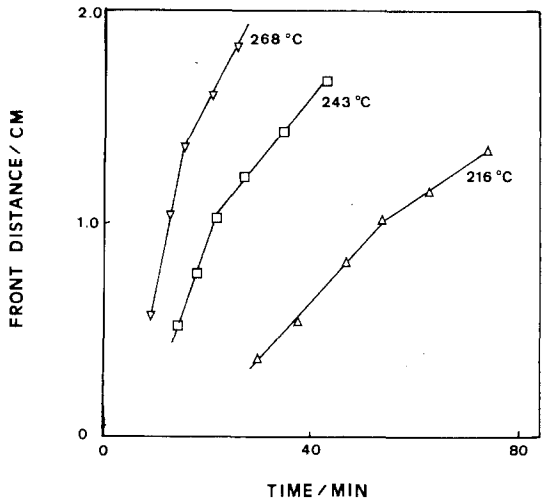

Fig. 4. Tungsten front distance vs. time at 90° (perpendicular to the direction of flow).

the wafer edge from 270° to 90°. Within a few minutes, a complete ring of tungsten had formed around the wafer edge. This ring continued to grow radially inward over the PI surface until a small circular area of tungsten-free PI remained. At this point the reaction was stopped. In each case the circular area of PI was located to the right of center (toward the reactor outlet) by about 1 cm. Plots of the tungsten film progress as a function of time and temperature are shown in Fig. 3 for both the upstream wafer edge (0°) and the downstream edge (180°). At 90° the film growth direction is perpendicular to the direction of flow. These growth progress results are shown in Fig. 4. Tungsten was never observed near the wafer center, inside of the advancing film front, during any of the runs. The set of photographs showing this deposition sequence for the 268°C run is shown in Fig. 5. A paper tracing/weighing technique was used to determine the fractional area of PI remaining at a given time during the deposition sequence. The fractional area covered by tungsten as a function of time is shown in Fig. 6.

Four-point probe sheet resistance measurements were made at numerous locations across the tungsten film on each wafer. The sheet resistance is lowest near the wafer edge and increases rapidly only near the tungsten/PI interface. The results of a set of measurements along an imagi-

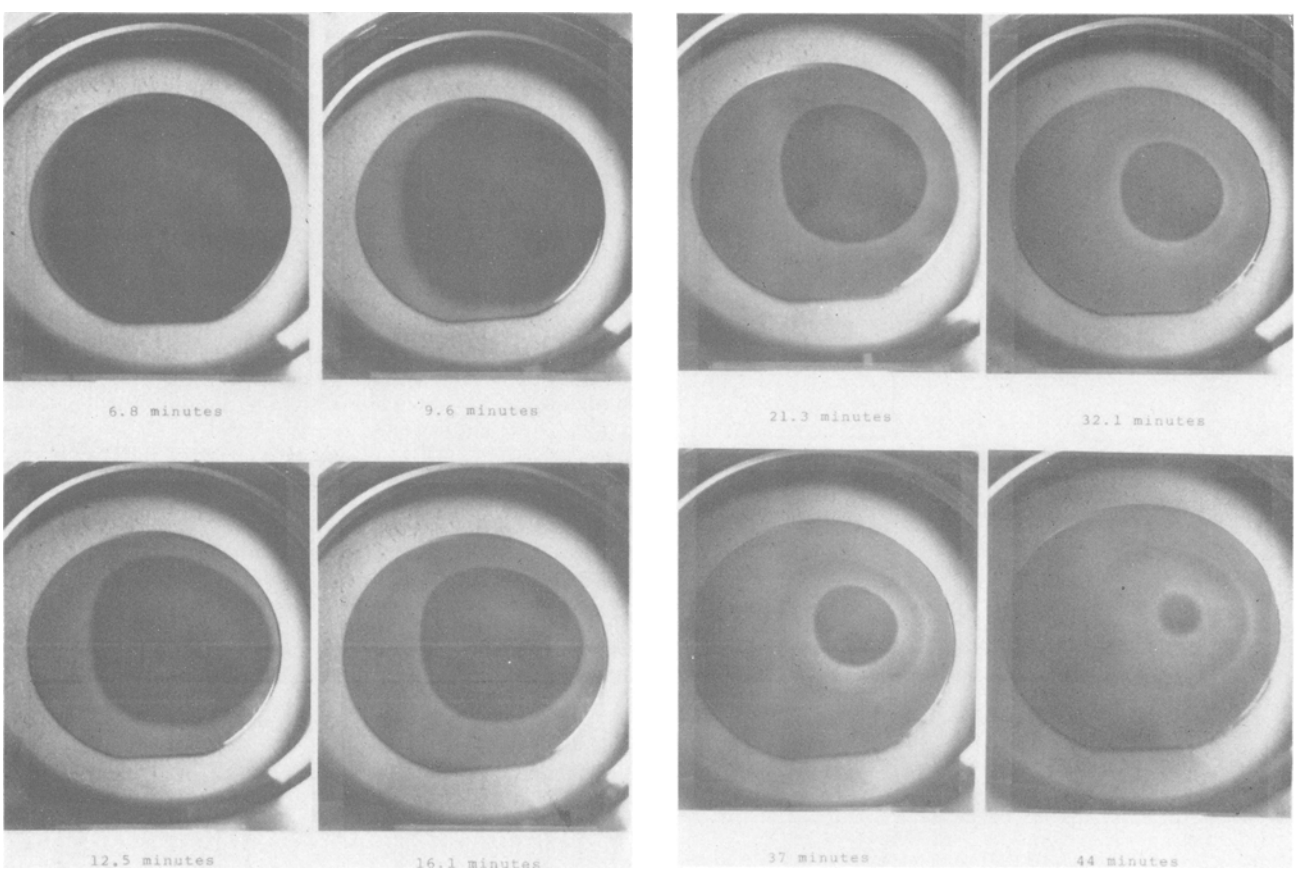

Fig. 5. Photographs of tungsten film growth on polyimide at 268°C

Downloaded on 2015-06-14 to IP 134.117.10.200 address. Redistribution subject to ECS terms of use (see ecsdl.org/site/terms_use) unless CC License in place (see abstract).

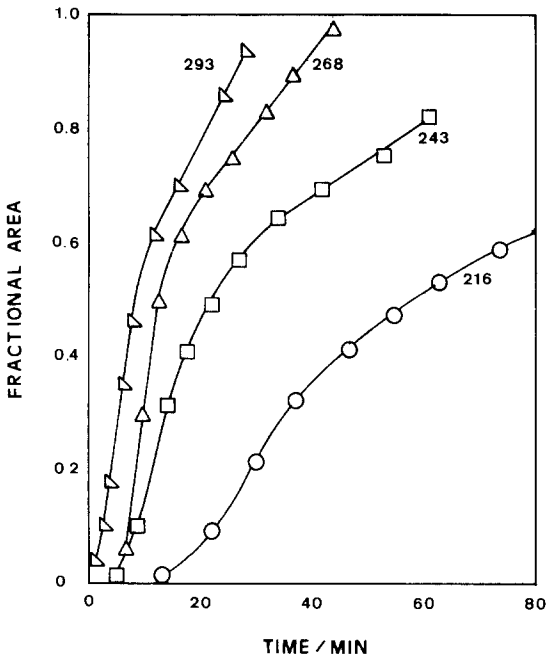

Fig. 6. Fractional wafer area covered by tungsten as a function of time and temperature.

nary x-axis from the 0° edge to the 180° edge (−3.8 to +3.8 cm) are shown graphically for the 243°C run in Fig. 7.

Discussion

The measured properties of the PI-2575-D cured films agree fairly well with values obtained from the manufacturer. The PI dielectric constant compares favorably with that of silicon dioxide, and is about half that of silicon nitride.

Although there are no reported values for PI-2575-D properties in the literature, Jensen (5), Senturia (16, 17), and Cech (18) have also observed linear relationships between moisture gain (or dielectric constant) and relative humidity for other polyimides. Senturia (17) reported a slope of the moisture gain-RH line of 0.021 weight percent (w/o) H_2O/%RH for a chemically similar du Pont PI, *vs.* 0.019 w/o H_2O/%RH for the PI-2575-D.

During the adhesion testing, one sample exhibited extensive adhesion loss after 2h in boiling water, whereas two other identically prepared samples did not. The one sample that exhibited this adhesion loss may have been anomalous. There appeared to be a small degree of adhesion loss after 2h in boiling water for the films cured at 440°C. Linde (19) studied the chemical bonding of APS aminosilane between polyimide and silicon dioxide. He found that APS begins to decompose at temperatures above approximately 400°C.

The PI-2575-D film appearance was excellent, with no color variations, striations, or fish eyes. Film thickness uniformity was also excellent. Thickness variations were almost within the limit of measurement on the Alpha-Step.

Based on the zero detectable mass gain of each polyimide-coated wafer in the selectivity experiments, it can be concluded that PI-2575-D polyimide films exhibit good selectivity from tungsten deposition. In other words, at 216°C in the absence of silicon or tungsten metal surfaces immediately adjacent to the polyimide film, tungsten will not deposit on PI-2575-D under a wide range of deposition times and pressures. The presence of hot tungsten surfaces more than 2 cm away from the PI film (*e.g.*, tungsten coated heating rods, underside of heating block) did not appear to affect selectivity.

In each of the deposition runs without the Teflon barrier, the nonselective tungsten deposition exhibited a definite radial dependence, with deposition moving in from the wafer edge with time. Based on this observation, the results from the selective depositions, and the findings of McConica (13), it is clear that the deposition of tungsten on a dielectric such as polyimide or SiO_2 is catalyzed by the presence of tungsten near the dielectric surface. An intermediate with a short diffusion length may possibly be formed from WF_6 and/or hydrogen on hot tungsten surface sites. This intermediate then diffuses to the PI surface, adsorbs or reacts, and creates a nucleation site for tungsten deposition.

It was observed that the area coverage rate of tungsten deposition on PI decreased with time. In the case of the front progress at 90° (Fig. 4) it can be seen that the plots can be fit with two lines. At distances less than 1 cm from the tungsten block the rate of progress of the front is much greater than at distances greater than 1 cm from the wafer edge. There is also a tendency for the slope change to move further in on the wafer as the temperature increases (Fig. 4). Plots of the fractional area covered with time show this same behavior (Fig. 6), with the center of slope change moving from 30% coverage at 216°C to 60% coverage at 293°C.

These observations can be explained by assuming that the progress of the front is due to an intermediate diffusing from the hot tungsten surface to the polyimide and then creating a new site for tungsten film growth. The fact that the upstream (0°) front rate is so much more rapid than the downstream rate (180°) is simply due to the intermediate having a gas phase lifetime and being carried by the convective flow. Depletion of the reactants is a minor effect at these temperatures since conversions are less than 1%. The fact that the intermediate is equally influenced by its local concentration gradient and convective flow is supported by a calculated Peclet number near unity for WF_6 at the reaction conditions.

The plots of fractional area covered should average out the convective effect because one-half of the wafer will experience enhanced front progress while the other half experiences retarded front progress.

The change in slope is due to the large temperature difference between the block and the wafer. At early times or coverages the primary source of the intermediate is the tungsten-covered substrate heater. At later times and coverages the front is moving due to intermediate created by the tungsten on the wafer which is 40°-90°C cooler than the block, depending upon the reaction conditions. Because the gas phase diffusivity and the rate of creation of the in-

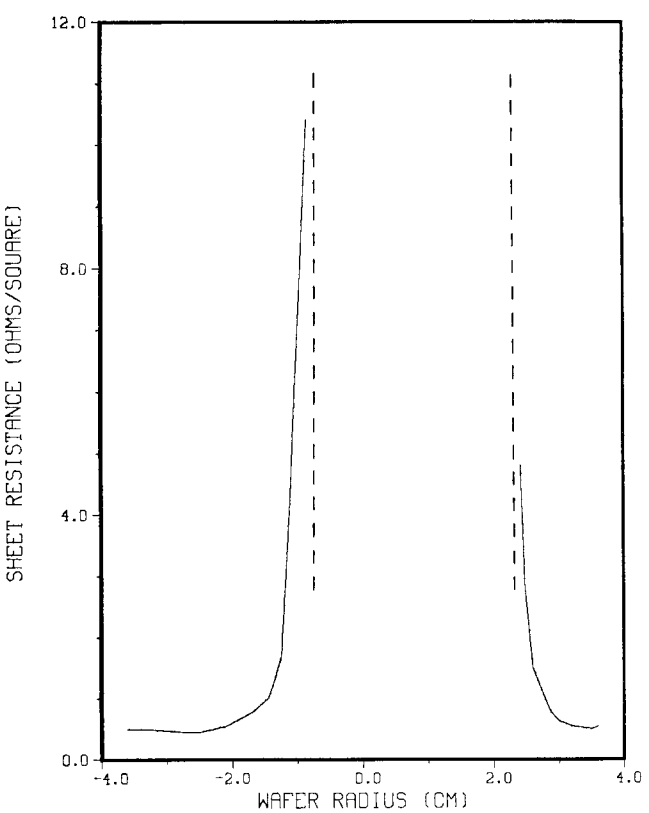

Fig. 7. Tungsten sheet resistance *vs.* location on wafer

Downloaded on 2015-06-14 to IP 134.117.10.200 address. Redistribution subject to ECS terms of use (see ecsdl.org/site/terms_use) unless CC License in place (see abstract).

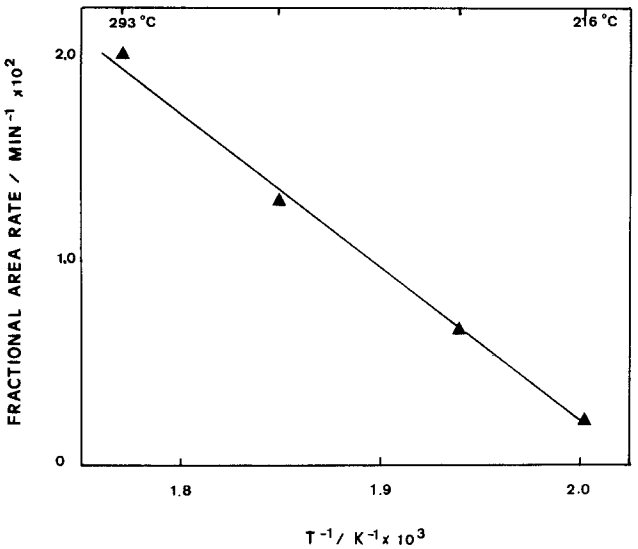

Fig. 8. Arrhenius plot of tungsten fractional area rate *vs.* inverse temperature.

termediate both increase with temperature, it is expected that the rate of front progress and the influence of the block intermediate generation on the wafer would increase with increasing temperature. An Arrhenius plot of the final tungsten coverage rates was made for the calibrated wafer temperatures (Fig. 8). An activation energy of 16 kcal/mol was measured (regression coefficient r^2 = 0.992). This activation energy is curiously close to the value of 17 kcal/mol reported by McConica (11) for the hydrogen reduction of WF_6. It is also well below the 25 kcal/mol reported by McConica and Cooper (13) for the creation of small tungsten nucleation sites on thermal oxide. The activation energy for film front progress is not expected to match that for nucleation, for they are not the same phenomena. Film progress inherently contains the diffusive effect of the intermediate which initiates nucleation.

The reactive intermediate which results in nucleation and film growth has a short lifetime as evidenced by the radial film growth. Its effect is not observed more than 0.5-1.0 cm from a hot tungsten surface. If nucleation occurs in the gas phase, it may be due to a subfluoride of tungsten (WF_x) disproportionating and giving a nonvolatile tungsten subfluoride (WF_{x-n}) which then condenses upon the polyimide creating a surface site for the hydrogen reduction reaction. These results on polyimide support the mechanism proposed by Creighton (22).

The shift of the remaining PI area became more pronounced at higher temperatures, ranging from 0.6 (260°C) to 1.3 cm (383°C). To differentiate between a depletion effect of the intermediate and a convective effect upon the displacement of the remaining PI area, the mass, momentum, and energy continuity equations would need to be solved. If a momentum boundary layer were present, the increased diffusivity of the reactive intermediate at higher temperature could allow it to further penetrate the flow field. This would result in an increase in the convective effect at higher temperatures.

The observed radial increase in tungsten film sheet resistance toward the wafer center, as shown in Fig. 7, is most likely due to a radial decrease in tungsten film thickness. Beinglass (7) observed an inverse log-log relationship between CVD tungsten sheet resistance and film thickness. Figure 5 illustrates that the tungsten film is of uniform thickness until the last 0.5-1.0 cm near the film front. The rate of tungsten film front growth is five orders of magnitude higher than the vertical deposition rate. This means that the deposition process is clearly due to tungsten nucleation on the polyimide, rather than just the lateral growth of tungsten on tungsten.

The nonselective tungsten films' adhesion to polyimide appeared to be excellent, but film stress was high enough to cause cracking, especially in the 268° and 293°C deposited films. This cracking was more pronounced near the wafer edge, especially near the 0° edge where the tungsten is thickest due to long deposition times. SEM analysis of one such crack showed that the tungsten film was so strongly adherent to the polyimide that the PI film was sheared as the tungsten film cracked. As a result, it appears that polyimide alone may not be a suitable dielectric for blanket tungsten deposition.

Conclusions

From the results of the physical and electrical property testing of the du Pont PI-2575-D, it can be stated that this material exhibits many of the desired properties of an interlevel dielectric: ease of processing; uniform film thickness; low dielectric constant and sufficiently high breakdown strength; and generally good adhesion to the underlying substrate. Its degree of water absorption is comparable to that of other PI's reported in the literature.

Under the conditions of 216°C and 0.75-7.5 torr total pressure, PI-2575-D films exhibit perfect selectivity in the absence of nearby tungsten surfaces. With the Teflon barrier removed, tungsten deposition was observed within a few minutes. This deposition exhibited a radial dependence; tungsten first appeared at the wafer edge, and the tungsten film front grew radially inward toward the center. An asymmetric behavior was observed during the deposition, *i.e.*, the moving tungsten film front was shifted toward the reactor outlet.

It was concluded that the deposition of tungsten on PI is catalyzed by nearby tungsten surfaces. The tungsten surface creates a gas phase reactive intermediate which diffuses to nearby polyimide surfaces creating a site for nucleation to occur, allowing film growth. The rate of film progress increases with temperature, as evidenced by an activation energy of 16 kcal/mol. Before a mechanism for tungsten nucleation and film growth can be proposed, these results will be modeled in terms of mass and momentum transfer. The current objective of this research group is to model tungsten film progress on polyimide and thermal oxide in terms of a traveling wave in order to find the real kinetic activation energy, with decoupled diffusive and convective effects.

The loss of selectivity on polyimide is similar to that observed on SiO_2; it results from a by-product of the hydrogen reduction reaction on tungsten rather than a reaction between the insulator, WF_6 and H_2. Like SiO_2, polyimide is inherently nonreactive and would be selective if the reaction creating the nucleating intermediate could be identified and suppressed. Examination of the selectivity of other polyimide materials and further characterization of the nonselective deposition is the subject of future work in this laboratory.

Acknowledgments

The authors acknowledge NCR Corporation and Sandia National Laboratories for funding this research and for their donation of materials. We would also like to thank du Pont Electronic Materials Division for their technical support and donation of polyimide materials, Genus Corporation for their donation of high purity tungsten hexafluoride, and Kirk Anderson and Mark Eaton for their help with sample preparation and analysis.

Manuscript submitted July 22, 1987; revised manuscript received Nov. 16, 1987.

REFERENCES

1. R. Iscoff, Semiconductor International, 116, October (1984).
2. T. O. Herndon and R. L. Burke, in Proc. Kodak Interface Conf., October 25-26, 1979.
3. P. Shah, D. Laks, and A. M. Wilson, in IEEE Proc. Intl. Conf. on Electrical Discharge Machining, 465 (1979).
4. S. Wolf and W. C. Atwood, U.S. Pat. 4,495,220 (1985).
5. R. J. Jensen, J. P. Cummings, and H. Vora, in *IEEE Trans. Components, Hybrids, Mfg. Technol.*, 384, December (1984).
6. N. Kakuda, T. Wada, N. Naito, and N. Mutoh, *IEEE Electron Device Lett.*, **6**, 589 (1985).
7. I. Beinglass, in "Tungsten and Other Refractory Metals for VLSI Applications," Albuquerque, NM, Oct. 7-9 (1985).
8. R. A. Levy, M. L. Green, P. K. Gallagher, and Y. S. Ali,

Downloaded on 2015-06-14 to IP 134.117.10.200 address. Redistribution subject to ECS terms of use (see ecsdl.org/site/terms_use) unless CC License in place (see abstract).

This Journal, **133,** 1905 (1986).
9. T. Moriya and H. Itoh, in "Tungsten and Other Refractory Metals for VLSI Applications," Albuquerque, NM, Oct. 7-9 (1985).
10. T. Moriya *et al.*, Extended Abstracts, 15th Conf. on Solid State Devices and Materials, Tokyo, Japan (1983).
11. C. M. McConica and K. Krishnamani, *This Journal*, **133,** 2542 (1986).
12. ASTM Test Method D-3359-76, 662 (1978).
13. C. M. McConica and K. J. Cooper, Submitted to *This Journal* (1987).
14. du Pont PI-2575-D Technical Bulletin (April 1986).
15. Y. Pauleau and Ph. Lami, *This Journal*, **132,** 2779 (1985).
16. D. D. Denton, D. R. Day, D. F. Priore, and S. D. Senturia, *J. Electron. Mater.*, **14,** 119 (1985).
17. D. D. Denton, J. B. Camou, and S. D. Senturia, Electrical Engineering Dept., MIT (1985).
18. J. M. Cech *et al.*, "Photoimageable Polyimide: A Dielectric Material for High Aspect Ratio Structures," Gould Research Center, Rolling Meadows, IL (1986).
19. H. Linde, *J. Polym. Sci. Polym. Chem. Ed.*, **22,** 3043 (1984).
20. C. N. Satterfield, "Heterogeneous Catalysis in Practice," McGraw-Hill, New York (1980).
21. W. F. Beadle, J. C. Tsai, and R. D. Plummer, "Quick Reference Manual for Silicon Integrated Circuit Technology," Wiley, New York (1985).
22. R. Creighton, "Tungsten and Other Refractory Metals for VLSI Applications 11," E. Broadbent, Editor, p. 43, MRS, Pennsylvania (1987).

Low Pressure Chemical Vapor Deposition of Tantalum Silicide

Glyn J. Reynolds*

Varian Research Center, Palo Alto, California 94303

ABSTRACT

A single wafer, cold wall, load-locked vacuum chamber with automated wafer handling capability was constructed for low pressure chemical vapor deposition of tantalum silicide. $TaSi_x$ was deposited at pressures between 100 mtorr and 1 torr over the temperature range 620°-700°C using mixtures of SiH_4, $TaCl_5$, H_2, HCl, and Ar. Stoichiometry could be controlled by adjusting temperature, pressure, and the partial pressures of reactant gases. Good adhesion on Si and SiO_2, and as-deposited resistivity values as low as 55 μΩ-cm were achieved. Films were analyzed by SEM, AES, RBS, and automated four-point probe. Impurity concentrations were below 0.5%, and deposition rates of 300-400 Å/min were observed.

Several transition metal silicides have been proposed for metallization in semiconductor applications. Of these, four refractory metal silicides, WSi_2, $MoSi_2$, $TaSi_2$, and $TiSi_2$ have received significant attention as candidate interconnect metals and in polycide gates (1).

The trend toward ever larger scale integration has been accompanied by a concomitant decrease in feature sizes, and it has become increasingly difficult for line-of-sight deposition methods such as sputtering or evaporation to adequately cover vertical sidewalls. Consequently, attention has been directed toward chemical vapor deposition as a means of achieving improved step coverage. There have been many reports in the literature of chemical vapor deposition of refractory metal silicides (2, 3), and commercial reactors are available for low pressure CVD of both WSi_x (4) and $TiSi_x$ (5).

In 1981, Murarka (6) expressed a preference for tantalum disilicide over the three other commonly used refractory metal disilicides. Shortly thereafter, Lehrer *et al.* (7, 8) described a hot wall batch process for LPCVD of tantalum silicide. Here, $TaCl_5$ and SiH_4 were reacted over the temperature range of 600°-650°C to yield a silicide close in stoichiometry to Ta_5Si_3. This layer was then annealed above 800°C, in order to cause reaction with an underlying predeposited polysilicon film. Silicon diffused from the polysilicon into the tantalum silicide, eventually converting it to the pure disilicide, $TaSi_2$. However, a TEM cross section of an annealed polysilicon/$TaSi_2$ bilayer film showed that the underlying polysilicon layer had been almost totally consumed in converting the metal-rich film to the disilicide. Furthermore, the silicon had diffused from the polysilicon to the tantalum silicide in a nonuniform manner; both the upper surface of the silicide and the silicide/polysilicon interface appeared rough. The authors concluded that a process to deposit stoichiometric $TaSi_2$ was required.

More recently, workers from Siemens have successfully deposited $TaSi_x$, $x \geq 2.0$. Two such processes were described; the first, a plasma-enhanced deposition, used $TaCl_5$ and SiH_2Cl_2 (9), and the second, a purely thermally activated process, used $TaCl_5$ and SiH_4 (10). Both processes were carried out in cold wall, single-wafer reactors. Other workers, using hot wall batch systems (11, 12), were unable to deposit the stoichiometric disilicide, in accordance with the earlier work of Lehrer and co-workers (7, 8).

In 1984, Murarka (13) listed the advantages and disadvantages of silicide deposition by chemical vapor deposition and indicated that CVD would be his preferred deposition method if it was technically feasible. Briefly, the advantages that he perceived for CVD silicides over their sputtered analogues were as follows: (*i*) good step coverage; (*ii*) high throughput; (*iii*) possible to deposit polysilicon and metal silicide in the same run; (*iv*) clean polysilicon/silicide interface; (*v*) lower processing temperature. He also listed several disadvantages; namely: (*i*) possible contamination from metal vapor; (*ii*) etching of the silicide which is already formed; (*iii*) rough surfaces.

The objective of this work was to deposit device-quality tantalum silicide films onto silicon or oxidized silicon substrates by LPCVD. Experimental apparatus was constructed to allow replication of the cold wall, single-wafer process reported by Wieczorek (10), whereby $TaCl_5$ and SiH_4 react in the presence of hydrogen on a heated substrate to yield $TaSi_x$. Special attention was given to provide a medium high vacuum system equipped with a load-lock, automated wafer handling and a turbomolecular pump which enabled base pressures below 10^{-6} torr to be attained.

Experimental

A block diagram of the equipment used is shown in Fig. 1. The wafer transport system was derived from the Varian-Gartek XM-8 sputter coating system. The reaction chamber and vacuum manifold were constructed from 304 stainless steel, and Viton O-rings or gaskets were used throughout. The Edwards Roots blower/rotary vane pump combination had a pumping speed of 600 cfm. The turbomolecular pump was a Leybold-Heraeus corrosion resistant 450C Model, with a pumping speed of 500 l/s, and was backed by an Alcatel rotary vane pump (27 cfm pumping speed). Both roughing pumps were equipped with Motor Guard oil filtration systems, and perfluorinated polyether vacuum pump fluids were used throughout. Either pumping package could be used for processing, al-

* Electrochemical Society Active Member.

Downloaded on 2015-06-14 to IP 134.117.10.200 address. Redistribution subject to ECS terms of use (see ecsdl.org/site/terms_use) unless CC License in place (see abstract).